Non-Steroidal Anti-Inflammatory Drug Induced Membrane Fusion: Concentration and Temperature Effects

ARTICLE *in* THE JOURNAL OF PHYSICAL CHEMISTRY B · DECEMBER 2009

Impact Factor: 3.3 · DOI: 10.1021/jp9069527 · Source: PubMed

2 AUTHORS:

Sutapa Mondal Roy
Sardar Vallabhbhai National Institute of Te…
11 PUBLICATIONS **90** CITATIONS
SEE PROFILE

Munna Sarkar
Saha Institute of Nuclear Physics
45 PUBLICATIONS **1,170** CITATIONS
SEE PROFILE

Non-Steroidal Anti-Inflammatory Drug Induced Membrane Fusion: Concentration and Temperature Effects

Sutapa Mondal and Munna Sarkar*

Chemical Sciences Division, Saha Institute of Nuclear Physics 1/AF, Bidhannagar, Kolkata-700064, India

Received: July 22, 2009; Revised Manuscript Received: October 20, 2009

Membrane fusion is a critical step in many biological events. The fusion process is always induced by different fusogenic agents of which proteins and peptides form the largest group. The mechanistic details of the fusion process vary depending on the nature of the fusogenic agents. However, membrane fusion induced by small drug molecules at physiologically relevant concentration has not been observed. Only recently our group has shown that three painkillers, namely, meloxicam, piroxicam, and tenoxicam, belonging to the oxicam group of non-steroidal anti-inflammatory drugs (NSAIDs) share this property. In this work, we present the effect of drug concentration and temperature on the kinetics of the fusion process. Small unilameller vesicles (SUVs) formed by dimyristoylphosphatidylcholine (DMPC) with an average diameter of 50−60 nm were used as model membranes. Fluorescence assays were used to probe the time dependence of lipid mixing, content mixing, and leakage whereas transmission electron microscopy (TEM) was used to image the fusion process and to calculate the average diameter of the vesicles. The results show that, in this fusion process, lipid mixing and content mixing are two sequential events and can occur even at a very low drug to lipid ratio (*D*/*L*) of 0.018. For a *D*/*L* ratio greater than 0.045, leakage of the vesicles leading to rupture compete with the fusion thereby inhibiting it. Temperature variation in the presence of drugs gives linear Arrhenius plots and is used to calculate the activation energies for the lipid mixing and content mixing, which are less compared to that seen in SUVs with a smaller diameter of 45 nm. Thermodynamic parameters of the transition state are calculated. The fusogenic property of the drugs has been interpreted in terms of the ability of the drugs to introduce membrane perturbation even at such low *D*/*L* ratios as studied here.

1. Introduction

Cellular membrane fusion is essential for many biological processes such as entry and exit of different molecules, viral infection,[1] fertilization,[2] etc. and intracellular fusion is essential in the extensive exo- and endocytosis at the level of the plasma membrane, mitochondrial remodeling, etc. These are controlled by different fusogenic agents of which proteins and peptides constitute the largest group.[3−5] Controlled membrane fusion has a wide range of applications in biotechnology and biomedical engineering.[6] It is an integral process in the production of hybridomas, which are formed by the fusion of dendritic and tumor cells,[7] in gene therapy for the transfer of therapeutic genome from the viral vector to the target cells,[8] and in nuclear transfer of round spermatids with oocytes or second polar body (PB-II) with male pronucleus for the fertility treatment and animal propagation.[9−11]

Fusogenic agents other than proteins and peptides are known to induce fusion in vitro.[12] Membrane fusion induced by small molecules other than cations such as Ca^{2+} is not common.[13] Cations, for example, Ca^{2+}, can induce fusion but only in anionic membranes where charge screening plays a crucial role.[14] Drug induced membrane fusion is a rare event that too occurring at physiologically relevant concentration of the drugs. Our group has shown that three painkillers belonging to the oxicam group of non-steroidal anti- inflammatory drugs (NSAIDs), namely, piroxicam (Px) [IUPAC name: (8*E*)-8-[hydroxy-(pyridin-2-ylamino)methylidene]-9-methyl-10,10-dioxo-10λ^6-thia-9-azabicyclo[4.4.0] deca-1,3,5-trien-7-one], tenoxicam (Tx) [IUPAC name: (3*E*)-3-[hydroxy(pyridin-2-ylamino)methylene]-2-methyl-2,3-dihydro-4*H*-thieno[2,3-*e*] [1,2]thiazin-4-one 1,1-dioxide], and meloxicam (Mx) [IUPAC name: (8*E*)-8-[hydroxy-[(5-methyl-1,3-thiazol-2-yl)amino] methylidene]-9-methyl-10,10-dioxo-10λ^6-thia-9-azabicyclo[4.4.0]deca 1,3,5-trien-7-one] (Figure 1), can induce membrane fusion at concentration relevant to the physiological concentration range, whereas NSAIDs belonging to other chemical groups do not share this new property.[15] A direct biological consequence of this fusogenic property of piroxicam is manifested in its ability to fuse and rupture the mitochondrial outer membrane leading to release of cytochrome C in the cytosol with the activation of the downstream proapoptotic caspase-3.[16]

Even though all membrane fusion is characterized by three major steps, namely, membrane contact, followed by lipid rearrangements to form the hemifusion state, and finally pore opening resulting in content mixing of the two cells or cell organelles,[17] the underlying mechanism varies with the nature of the fusogenic agent. Protein induced membrane fusion and drug induced membrane fusion in the absence of proteins are expected to have a different mechanism. Unraveling the mechanistic detail of these NSAIDs induced fusions will allow better use of these painkillers to induce fusion in a controlled manner as is necessary in many biotechnological/biomedical procedures.

As a step toward understanding the mechanistic details of NSAIDs, namely, Px, Tx, and Mx induced membrane fusion, in this work, we have studied the effect of drug concentration and temperature on the kinetics of the fusion process. Small

* To whom correspondence should be addressed. Fax: +91-33-23374637. Email: munna.sarkar@saha.ac.in.

10.1021/jp9069527 CCC: $40.75
Published on Web 12/02/2009

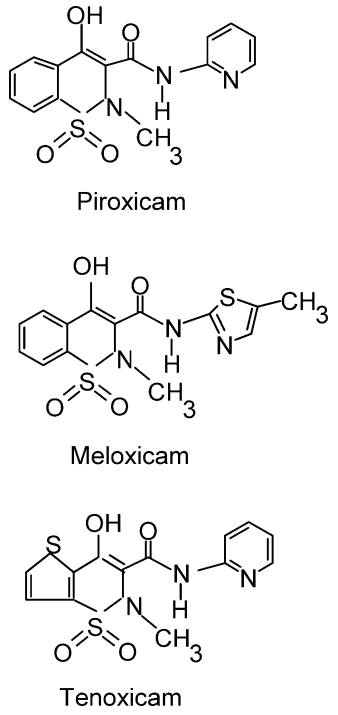

Figure 1. Chemical structures of piroxicam, meloxicam, and tenoxicam.

unilamellar vesicles (SUVs) formed by the phospholipids dimyristoylphosphatidylcholine (DMPC) were used as a model membrane. We are aware that DMPC as a membrane mimetic does not perfectly represent a biological membrane. However, we have chosen this simple model system as the starting model in deciphering the mechanism of NSAIDs induced membrane fusion due to various factors that are explained as follows. The headgroup of DMPC being zwitterionic in nature, there is no net charge on it, and it is expected to give the same advantage to a negatively or positively charged drug molecule. It is also the principal lipid component of mitochondria. It should be mentioned that at physiological pH of 7.4, all three oxicam NSAIDs are in their anionic form. DMPC having a C14 chain is expected to be disturbed by the incorporation of bulky oxicam NSAIDs. However, this is not the only reason behind the fusion process. We have already shown that incorporation of a NSAID with bulkier chemical structure such as indomethacin does not induce fusion of DMPC vesicles of the same size and under the same experimental condition as in the present study[15] Carefully designed control experiments without the drugs show that, despite relatively high curvature of the SUVs, spontaneous fusion of the vesicles was insignificant under the experimental conditions studied and within the time range covered. To monitor the time course of the three major events in the fusion process, namely, lipid mixing, content mixing, and leakage, three different fluorescence assays were used. Content mixing and leakage were monitored by the Tb^{3+}/DPA assay whereas lipid mixing was monitored using the standard N-NBD-PE/N-Rh-PE assay at physiological pH of 7.4. Kinetic parameters were extracted from the time courses of the change in fluorescence intensity of the probes used in the different assays, both as a function of drug concentration and temperature variation. Arrhenius plots were used to calculate the activation energy of the different steps from which the thermodynamic parameters of the transition state could be estimated. Transmission electron microscopy (TEM) was used to image the vesicles at the different stages of the fusion process and to calculate the average diameter of the SUV at different drug concentrations.

2. Material and Methods

Dimyristoylphosphatidylcholine (DMPC), TritonX-100 (ultra pure), dipicolinic acid (DPA), terbium (Tb^{3+}) chloride, Px, and Tx were purchased from Sigma-Aldrich (St. Louis, MO), Mx from LKT Laboratories (St. Paul, MN), N-NBD-PE [*N*-(7-nitrobenz-2-oxa-1,3-diazol-4-yl)-1,2-dihexadecanoyl-*sn*-glycero-3-phosphoethanolamine, triammonium salt] and N−Rh−PE (Lissamine rhodamine B-1,2-dihexadecanoyl-*sn*-glycero-3-phosphanolamine, triethylammonuim salt) from Invitrogen Life Science Corporation (Carlsbad, CA), 2-[tris(hydroxymethyl)-methylamine]-1-ethanesulfonic acid (TES buffer) and sodium ethylene diamine tetra aceate (EDTA sodium salt) were purchased from SRL (India), and all were used without further purification. Water was quartz distilled thrice before use. Stock solutions of the NSAIDs were prepared in dimethyl sulfoxide (DMSO) (Merck, Germany), and the exact concentration was adjusted by the corresponding buffer. The dilution of the drugs was done in such a way so that each sample contains 0.5% (v/v) of DMSO. It should be mentioned that the presence of 0.5% (v/v) of DMSO had no effect on the vesicles, and this has been verified from the TEM images of the vesicles in the presence and absence of 0.5% (v/v) DMSO (data not shown). Also, 0.5% (v/v) DMSO itself did not have any effect on the fusion process and has been included in all the control experiments where fusion was monitored in absence of the drugs.

2.1. Preparation of SUVs. Small unilamellar vesicles (SUVs) of DMPC were prepared by the method of sonication.[18] To prepare SUVs of DMPC, the phospholipid was dissolved in 2:1 (v/v) chloroform/methanol solution, and the solvent was evaporated under a stream of argon. The resultant lipid film was then dried overnight in a vacuum desiccator at −20 °C. The dried film was hydrated and swelled in 10 mM 2-[tris(hydroxymethyl)-methylamine]-1-ethanesulfonic acid (TES) and 60 mM NaCl at pH 7.4 for $TbCl_3$ (8 mM) containing vesicles and 10 mM TES at pH 7.4 for dipicolinic acid (DPA) (80 mM) vesicles. For N-NBD-PE and N-Rh-PE containing vesicles, 10 mM TES and 60 mM NaCl at pH 7.4 was used to hydrate the lipid films. The mixture was vortexed to disperse the lipids. The dispersion was then sonicated for about 10 min using a dr. Heilscher (Germany) probe sonicator (200 W). The samples were then allowed to stand for 40 min at 37 °C to be hydrated completely. The sonicated samples were centrifuged at 10 000 rpm for 15 minutes to remove titanium particles and aggregated lipids.[19] The titanium particles were introduced as an impurity in the sample from the sonicator probe.

2.2. Estimation of Phosphate. The phospholipid concentration was measured by following the published protocol.[20] Vesicle samples of 0.2 mL were digested with 0.8 mL of perchloric acid at 180 °C for 3 h. After cooling to room temperature, 5.0 mL of distilled water was added to it. Ammonium molybdate solution (5%, 0.5 mL) was then added followed by addition of 0.4 mL of aminonaphthol sulfonic acid (ANSA) reagent (prepared by dissolving 6 mg of sodium metabisulfate, 1.2 mg of sodium sulfite, and 100 mg of ANSA in 50 mL of distilled water). A blue color was allowed to develop for 20 minutes, and the amount of phosphate was estimated from the absorbance measured at 660 nm using a Shimadzu UNICAM-UV-500 absorption spectrophotometer.

2.3. Content Mixing Assay. The Tb/DPA (terbium chloride−dipicolinic acid) content mixing assay was based on those originally proposed and modified by Wilschut et al.[21,22] Vesicles were prepared in either 80 mM DPA or 8 mM $TbCl_3$, and the untrapped probes, present in the external buffer of the vesicles,

were removed using a Sephadex G-50 (Amersham Biosciences) column equilibrated with assay buffer (10 mM TES, 100 mM NaCl, 1 mM EDTA at pH 7.4). The lipid concentration in all the experiments was kept at 1.1 mM as determined by the phosphate estimation method (data not shown).

To monitor drug induced content mixing, requisite amount of stock drug solutions were added to a (1:1) mixture of Tb^{3+} and DPA-containing vesicles, and the time course of the content mixing were measured in terms of an increase in fluorescence intensity at 490 nm, due to the formation of the highly fluorescent Tb/DPA complex, which is excited at 275 nm. To calibrate the fluorescent scale (100% content mixing), an aliquot of chromatographed Tb-vesicles was rechromatographed on a Sephadex G-50 column and equilibrated with 10 mM TES, 100 mM NaCl, pH 7.4 to eliminate the EDTA in the first buffer so that the released Tb^{3+} from the vesicles would not be chelated.[22] An aliquot of rechromatographed Tb-vesicles was lysed by 0.1% (w/v) Triton X-100 in the presence of an adequate amount of DPA, avoiding excess addition. The released Tb^{3+} will be fully complexed with DPA, which was assumed to be 100% content mixing. Then, the percent of content mixing was calculated in the following way:

$$\% \text{ Content Mixing} = \frac{(F - F_0)/F_0}{(F^l - F_0^l)/F_0^l} \times 100 \qquad (1)$$

where F is the fluorescence intensity of the Tb/DPA complex in the presence of drug at time t, F_0 is the fluorescence intensity of the Tb/DPA complex in the presence of drug at $t = 0$, F^l is the fluorescence intensity of rechromatographed, lysed Tb-vesicles in the presence of an adequate amount of DPA, and F_0^l is the fluorescence intensity of rechromatographed, lysed Tb-vesicles.

2.3.1. Concentration-Dependent Study. For the concentration-dependent study, the content mixing assay was done using varying concentration of all the oxicam NSAIDs with concentrations ranging from 20 to 150 μM with *D*/*L* ratios from 0.018 to 0.136. All the fluorescence measurements were done with a Jobin Yvon Spex Fluoromax3 operated in L-format and at a constant temperature of 37 °C.

2.3.2. Temperature-Dependent Study. For the temperature-dependent study, the content mixing assay was done using varying temperatures, namely, 27, 32, 37, and 42 °C. All the fluorescence data were measured in the Jobin Yvon Spex Fluoromax3 operated in L-format and at a constant concentration for all the oxicam NSAIDs at 30 μM, that is, the *D*/*L* ratio being at 0.027.

2.4. Leakage Assay. The leakage assay was done by using coencapsulated Tb/DPA vesicles.[12] Tb^{3+} (8 mM) and DPA (80 mM) coencapsulated vesicles, prepared in 10 mM TES, pH 7.4, were chromatographed on a Sephadex G-50 column equilibrated with 10 mM TES, 100 mM NaCl, and 1 mM EDTA at pH 7.4 to eliminate unbound probe in the external buffer. In the presence of drugs, when leakage of contents (coencapsulated Tb/DPA) occurs, there was a drop in fluorescence intensity due to the quenching of the Tb by EDTA in the external buffer. The concentration of all the oxicam NSAIDs was varied from 20 to 150 μM, that is, *D*/*L* ratios from 0.018 to 0.136. The decrease in fluorescence was measured at 490 nm with an excitation wavelength at 275 nm, and the fluorescence intensity was measured in a Jobin Yvon Spex Fluoromax3. The loss of remaining contents could be induced by addition of 0.1% (w/v) Triton X-100. 0% leakage was characterized by the fluorescence intensity of vesicles containing coencapsulated Tb/DPA in buffer with drug at $t = 0$; 100% leakage was characterized by the fluorescence intensity of a coencapsulated Tb/DPA vesicle sample treated with drug and 0.1% (w/v) Triton X-100. Both measurements were made relative to the fluorescence intensity of detergent released vesicles. Thus the percent leakage was calculated as

$$\% \text{ Leakage} = \frac{(F_{CO}^{d,t} - F_{CO}^{d,\text{det}}) - (F_{CO}^{d,t} - F_{CO}^{d,\text{det}})}{F_{CO}^{d,t=0} - F_{CO}^{d,\text{det}}} \times 100 \qquad (2)$$

where $F_{CO}^{d,t=0}$ is the fluorescence intensity of Tb/DPA coencapsulated vesicles in the presence of drug at the time $t = 0$ (first data in the kinetics measurement), $F_{CO}^{d,t}$ is the fluorescence intensity of Tb/DPA coencapsulated vesicles in the presence of drug with time, and $F_{CO}^{d,\text{det}}$ is the fluorescence intensity of Tb/DPA coencapsulated vesicles in the presence of drug after treatment of 0.1% (w/v) Triton X-100.

2.5. Lipid Mixing Assay. For measuring the rate of lipid mixing during drug induced membrane fusion, a fluorescence resonance energy transfer (FRET) assay was used as described previously.[23,24] For the assay, both the FRET pair of probes N-NBD-PE (donor) and N-Rh-PE (acceptor) were used at concentrations of 0.8 mol % each, in the probe containing vesicles. Two sets of vesicles, probe containing and probe free, were prepared in 10 mM TES, 100 mM NaCl, and 0.1 mM EDTA buffer at pH 7.4. The probe containing vesicles were mixed with probe free vesicles at a ratio of 1:9 and loaded in a quartz fluorescence cell. The fluorescence was monitored using a Hitachi F7000 spectrofluorometer with excitation at 460 nm and emission at 530 nm. In particular, the fluorescence dequenching of N-NBD-PE due to fusion was monitored with time. The fluorescence data were taken at a constant concentration of the oxicam NSAIDs at 30 μM, that is, a *D*/*L* ratio at 0.027, and with varying temperatures, namely, 32, 37, 42, and 50 °C. The oxicam drugs have some quenching effect on the fluorescence intensity of the lipid probes. This quenching effect was monitored by mixing probe containing vesicles with the buffer in the same dilution as it would be in the working solution mentioned above. Absence of probe free vesicles will ensure that fusion, even if it occurs in the presence of the drugs between probe containing vesicles, will not increase the resonance energy transfer (RET) distance between the probes. This will keep the value of FRET more or less constant, and the quenching effect of the drugs on the fluorescence intensity of the donor probes will be the dominant effect. The quenching of the fluorescence intensity was monitored in the same time range that was covered in the actual fluorescence experiment. The decrease in the fluorescence intensity at each time point is added to the fluorescence intensity in the original data to nullify the effect of fluorescence quenching to get the actual fluorescence intensity (F) for lipid mixing. The initial fluorescence of the labeled liposomes was recorded as 0% fluorescence, and 100% fluorescence was determined by lysing the vesicles with Triton X-100 at 1% (v/v) to the final concentration. This treatment will eliminate energy transfer and the signal yields the N-NBD-PE fluorescence obtained at infinite dilution. This is set to be the maximal (or 100%) fluorescence to calibrate the scale for the determination of percentage (%) lipid mixing. The ultrapure Triton X-100 used here does not affect the N-NBD-PE fluorescence; hence, the correction factor of 1.4−1.5 was not used.[25]

The lipid mixing is given by the following equation:

$$\% \text{ Lipid Mixing} = \frac{F - F_0}{F_\infty - F_0} \times 100 \quad (3)$$

where F is the fluorescence intensity at time t, F_0 is the residual fluorescence intensity, and F_∞ is the maximal (or 100%) fluorescence intensity.

Each experiment is repeated at least 3−4 times, and the error bar in the data points represents the standard deviation of that data point.

2.6. Transmission Electron Microscopy (TEM) Measurement. TEM was done with a FEI electron microscope model Tecnai G2 20S Twin operating at 200 kV with a resolution of 0.2 nm. Samples were spread over a copper grid coated with carbon. SUVs were negatively stained with 2% (v/v) phosphotungstic acid (PTA). The magnifications were varied from 15 000× to 19 500× for different samples, which are mentioned on the transmission electron micrographs.

3. Results

In Figure 2a, the representative time courses for content mixing, leakage, and lipid mixing are shown in the presence of 30 μM (D/L = 0.027) of Mx (i), Px (ii), and Tx (iii) at temperature 37 °C and pH 7.4. All the time courses could be fitted to a single exponential macroscopic rate equation [$f = a(1 - \exp(-kt))$], where the exponential constant k referred to as the rate constant, the extent of percent content mixing at infinite time is given by the pre-exponential factor a. In all three assays, that is, content mixing, leakage, and lipid mixing, control spectra were taken within the same time frame as that of the experiment to show that no fusion event is occurring in the studied time frame of the experiment in absence of the oxicam drugs, even though the size of the vesicles are small (diameter 50−60 nm determined from TEM study). For all three assays, the rate constant of fusion process in the presence of Mx always

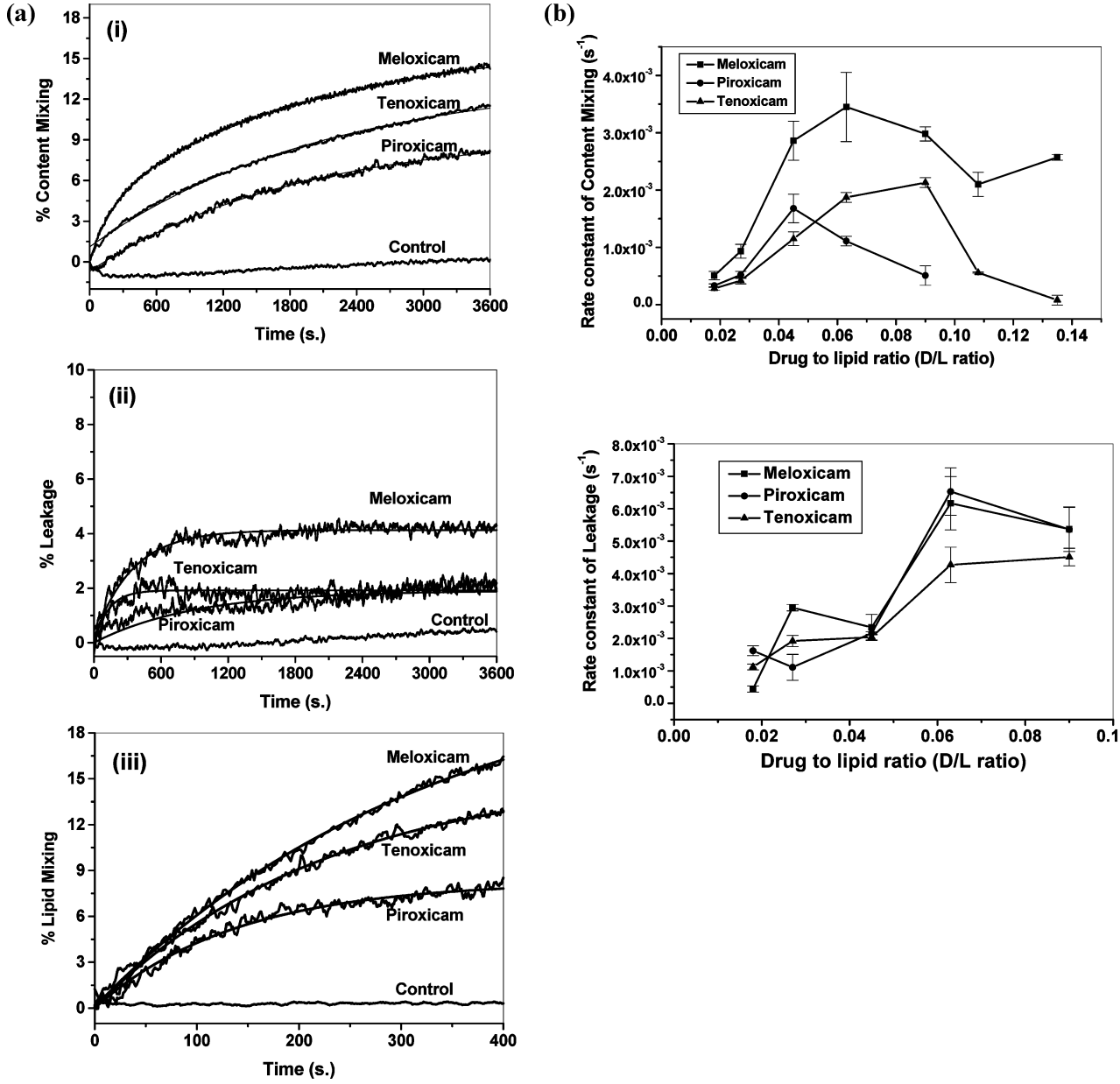

Figure 2. (a) Drug-dependent content mixing assay followed by Tb/DPA assay (i); leakage followed by Tb/DPA assay (ii); and lipid mixing followed by N-NBD-PE/^{N}Rh-PE assay (iii); of DMPC vesicles with time for meloxicam, tenoxicam, and piroxicam with a D/L ratio of 0.027 for all the drugs. The time courses were fit to single exponential curves [$f = a(1 - \exp(-kt))$] using Origin 7.0. The temperature was kept constant at 37 °C throughout the experiments. (b) Rate constants for content mixing and rate constants for leakage with varying drug to lipid ratios (D/L ratio) of the three oxicam NSAIDs. The temperature was kept constant at 37 °C for all the experiments.

TABLE 1: Rate Constants of Content Mixing and Leakage at Various Concentrations of Oxicam Drugs, Namely, Mx, Px, and Tx[a]

drug to lipid ratio (*D*/*L*)	rate constant (k in s^{-1}) at 37 °C		
	meloxicam	piroxicam	tenoxicam
	content mixing assay		
0.018	0.51×10^{-3} ($\pm 7.37 \times 10^{-5}$)	0.33×10^{-3} ($\pm 3.05 \times 10^{-5}$)	0.28×10^{-3} ($\pm 2.89 \times 10^{-5}$)
0.027	0.93×10^{-3} ($\pm 1.20 \times 10^{-4}$)	0.52×10^{-3} ($\pm 6.25 \times 10^{-5}$)	0.42×10^{-3} ($\pm 5.57 \times 10^{-5}$)
0.045	2.86×10^{-3} ($\pm 3.40 \times 10^{-4}$)	1.68×10^{-3} ($\pm 2.50 \times 10^{-4}$)	1.15×10^{-3} ($\pm 1.20 \times 10^{-4}$)
0.063	3.45×10^{-3} ($\pm 6.04 \times 10^{-4}$)	1.11×10^{-3} ($\pm 8.20 \times 10^{-5}$)	1.87×10^{-3} ($\pm 8.62 \times 10^{-5}$)
0.09	2.98×10^{-3} ($\pm 1.23 \times 10^{-4}$)	0.51×10^{-3} ($\pm 1.70 \times 10^{-4}$)	2.13×10^{-3} ($\pm 8.48 \times 10^{-5}$)
0.108	2.10×10^{-3} ($\pm 2.10 \times 10^{-4}$)		0.56×10^{-3} ($\pm 1.00 \times 10^{-5}$)
0.135	2.57×10^{-3} ($\pm 5.00 \times 10^{-5}$)		0.08×10^{-3} ($\pm 8.61 \times 10^{-5}$)
	leakage assay		
0.018	0.44×10^{-3} ($\pm 9.55 \times 10^{-5}$)	1.62×10^{-3} ($\pm 1.50 \times 10^{-4}$)	1.12×10^{-3} ($\pm 9.00 \times 10^{-5}$)
0.027	2.95×10^{-3} ($\pm 9.99 \times 10^{-5}$)	1.11×10^{-3} ($\pm 4.00 \times 10^{-4}$)	1.92×10^{-3} ($\pm 1.70 \times 10^{-4}$)
0.045	2.34×10^{-3} ($\pm 4.00 \times 10^{-4}$)	2.16×10^{-3} ($\pm 5.00 \times 10^{-5}$)	2.04×10^{-3} ($\pm 9.00 \times 10^{-5}$)
0.063	6.17×10^{-3} ($\pm 8.22 \times 10^{-4}$)	6.53×10^{-3} ($\pm 7.31 \times 10^{-4}$)	4.27×10^{-3} ($\pm 5.46 \times 10^{-4}$)
0.09	5.37×10^{-3} ($\pm 6.90 \times 10^{-4}$)	5.36×10^{-3} ($\pm 6.78 \times 10^{-4}$)	4.51×10^{-3} ($\pm 2.70 \times 10^{-4}$)

[a] In all experiments, the lipid concentration was 1.1 mM. Temperature and pH were kept constant at 37 °C and 7.4, respectively, throughout the experiments.

shows a maximum value whereas that in the presence of Tx is minimal. Px has an intermediate effect in terms of rate constants of fusion for various drug concentrations and temperatures.

3.1. Effect of Drug Concentration on Kinetics of Fusion. The effect of varying drug concentrations on fusion kinetics was studied in the case of content mixing, which marks the end of the fusion process. Our earlier data showed that all three oxicam NSAIDs, namely, Mx, Px, and Tx, have differential rates of content mixing and leakage though they are of the same genre with Mx showing the maximum rate and extent for content mixing with Tx showing the lowest.[15] The time courses for content mixing and leakage in presence of oxicam NSAIDs with *D*/*L* ratios 0.018, 0.027, 0.045, 0.063, 0.090, 0.108, and 0.135 all are fitted using a single exponential rate equation as shown earlier (plots not shown). The results for concentration dependent content mixing and leakage rates are given in Table 1 and plotted in Figure 2b. It is evident from the plots that, for all three oxicam NSAIDs, content mixing follows a general trend where the rate constants of content mixing increases with an increasing *D*/*L* ratio of the drugs and reaches a maximum value at a particular *D*/*L* ratio that is different for the three drugs. Beyond this *D*/*L* ratio, the rate constant starts decreasing with increasing drug concentration. The maximum rate is shown by Px, Mx, and Tx at *D*/*L* ratios of 0.045, 0.063, and 0.090, respectively. The variation of leakage rates with increasing *D*/*L* ratio clearly shows that, for all three drugs, the regions where the rate constants of content mixing are decreased, the rate constants of leakage have very high values. There is a sharp increase in the leakage rates beyond a *D*/*L* ratio of 0.045 with Px showing the highest rate followed by Mx and Tx. Since leakage predominates at higher drug concentrations, there is a fare chance for the lipid vesicles to get ruptured. Rupturing of the membranes of the lipid vesicles in the presence of high concentration of drugs (*D*/*L* ratios from 0.063 to 0.135) would inhibit the fusion process thereby reducing the rate of content mixing.

3.2. TEM Study To Prove Rupture. Transmission electron micrographs (Figure 3a) were taken using DMPC vesicles treated with 70 μM (*D*/*L* = 0.063) of Mx, Px, and Tx. The control was done by taking images of DMPC vesicles under identical experimental conditions but without added drugs. From Figure 2b, it is evident that, in the presence of 70 μM (i.e., *D*/*L* = 0.063), Mx shows maximum fusion, and for Tx, the fusion event is at its penultimate stage whereas for Px the fusion is on the decline, overwhelmed by the leakage or rupture. The TEM images show that, compared to the control, Mx treated vesicles show much larger diameters (Figure 3a (ii)) of already fused vesicles. The effect of Px on DMPC vesicles is seen in Figure 3a (iii) where significant white patches, the mark of ruptured membranes, are observed. Various fusion bodies along with large sized vesicles are seen in Figure 3a (iv) for Tx treated vesicles. The frequency distribution study based on the TEM slides (average was taken from four slides for each drug and control) shows (Figure 3b) that the drug untreated control has vesicles with an average diameter of 50−60 nm. In the presence of Mx, the average vesicle diameter is increased almost 2-fold as compared to the control with values in between 120 and 140 nm. This is consistent with Figure 2a that shows for Mx at a *D*/*L* ratio of 0.063 the fusion event maximizes and the presence of the maximum number of fused vesicles is reflected in the 2-fold increase of the average vesicle diameter. As mentioned before, at this *D*/*L* ratio, for Tx treated vesicles, the fusion event has not maximized showing average diameter between 70 and 80 nm (Figure 3b). For Px, as expected, the average vesicle diameter shows a decrease compared to the control, and the value is in between 40 and 50 nm. This decrease in vesicle size conclusively proves the occurrence of ruptured vesicles at higher concentration of oxicam NSAIDs. Figure 3a and 3b establishes the fact that the decrease in the content mixing rate indicates a decrease in the fusion event due to competitive leakage leading to rupture of the vesicles at higher drug concentration.

3.3. Temperature-Dependent Study of Lipid Mixing and Content Mixing: Arrhenius Plot. Both the content mixing and lipid mixing assays were done at four different temperature points, namely, 27, 32, 37, and 42 °C, drug concentration being constant at 30 μM (*D*/*L* = 0.027), and pH = 7.4. Above 50 °C, leakage highly predominates so that it overwhelms both content mixing and lipid mixing and that is why they could not be measured significantly. The plots for the lipid mixing and content mixing in presence of the three oxicam NSAIDs could be fitted to a single exponential rate equation as has been used earlier. All the rate constants for lipid mixing and content mixing in the presence of the three oxicam drugs at four temperatures are shown in Table 2. The respective Arrhenius plots are given in Figure 4a and b. The calculated activation energy of lipid mixing during membrane fusion has lower values compared to those of the activation energy for the content mixing process for Mx and Tx and comparable for Px (Table 3). Since lipid mixing has a lower activation barrier than content mixing, it is

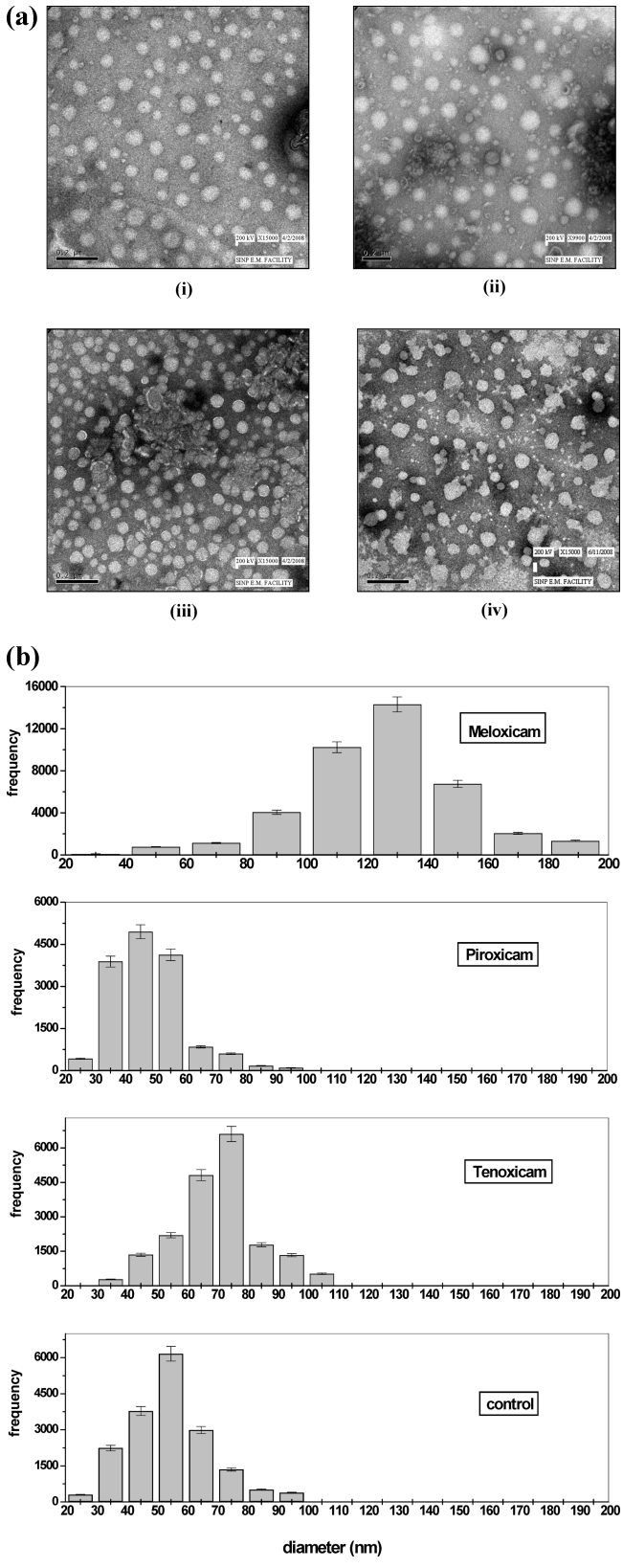

Figure 3. (a) Transmission electron micrographs of untreated DMPC vesicles (control) (i), DMPC vesicles treated with 70 μM (i.e., D/L = 0.063) of meloxicam (ii), piroxicam (iii), and tenoxicam (iv). In all cases, grids were prepared after 20 min of drug addition and stained with phosphotungstic acid (PTA). (b) Frequency distribution with respect to diameter of DMPC vesicles on treatment with oxicam NSAIDs (D/L = 0.063) at 37 °C and pH 7.4, calculated from TEM micrographs. For calculation, at least four micrographs of each sample were used.

TABLE 2: Rate Constants of Content Mixing and Lipid Mixing at Various Temperature and in the Presence of Three Oxicam Drugs, Namely, Mx, Px, and Tx[a]

temperature (°C)	rate constant (k in s^{-1})					
	lipid mixing assay			content mixing assay		
	meloxicam	piroxicam	tenoxicam	meloxicam	piroxicam	tenoxicam
27				0.230×10^{-3} ($\pm 0.064 \times 10^{-3}$)	0.325×10^{-3} ($\pm 0.007 \times 10^{-3}$)	0.165×10^{-3} ($\pm 0.049 \times 10^{-3}$)
32	1.775×10^{-3} ($\pm 0.091 \times 10^{-3}$)	5.250×10^{-3} ($\pm 1.690 \times 10^{-3}$)	2.125×10^{-3} ($\pm 0.417 \times 10^{-3}$)	0.365×10^{-3} ($\pm 0.021 \times 10^{-3}$)	0.400×10^{-3} ($\pm 0.014 \times 10^{-3}$)	0.280×10^{-3} ($\pm 0.021 \times 10^{-3}$)
37	2.445×10^{-3} ($\pm 0.035 \times 10^{-3}$)	7.800×10^{-3} ($\pm 1.500 \times 10^{-3}$)	4.650×10^{-3} ($\pm 0.325 \times 10^{-3}$)	0.933×10^{-3} ($\pm 0.12 \times 10^{-3}$)	0.520×10^{-3} ($\pm 0.006 \times 10^{-3}$)	0.420×10^{-3} ($\pm 0.056 \times 10^{-3}$)
42	4.600×10^{-3} ($\pm 0.036 \times 10^{-3}$)	7.110×10^{-3} ($\pm 1.580 \times 10^{-3}$)	5.120×10^{-3} ($\pm 0.707 \times 10^{-3}$)	1.105×10^{-3} ($\pm 0.122 \times 10^{-3}$)	0.720×10^{-3} ($\pm 0.042 \times 10^{-3}$)	0.590×10^{-3} ($\pm 0.097 \times 10^{-3}$)
50	9.310×10^{-3} ($\pm 0.051 \times 10^{-3}$)	15.160×10^{-3} ($\pm 2.101 \times 10^{-3}$)	8.220×10^{-3} ($\pm 0.675 \times 10^{-3}$)			

[a] In all the experiments, the D/L ratio was kept constant at 0.027 and pH was 7.4.

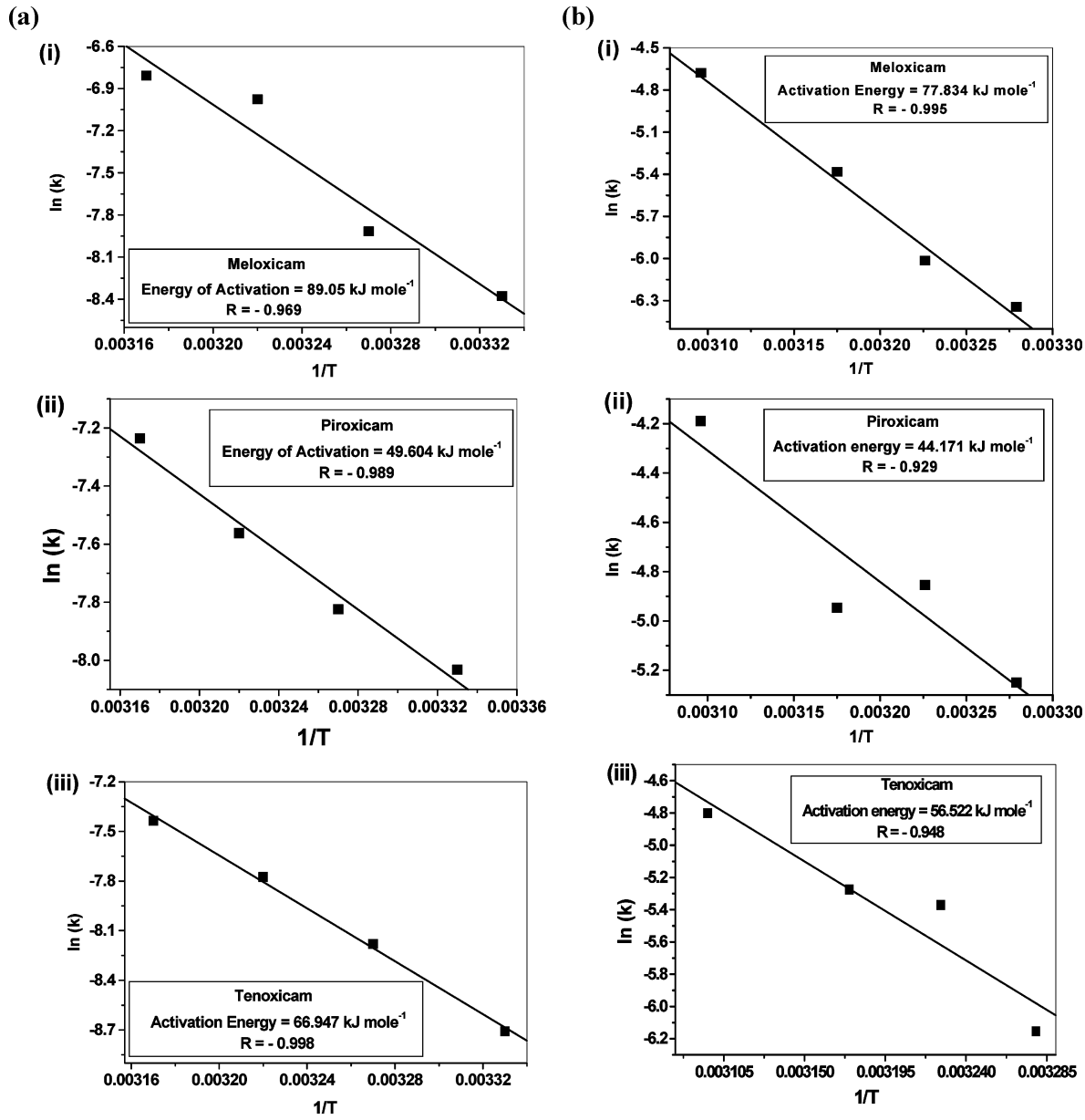

Figure 4. (a) Arrhenius plots of content mixing at *D*/*L* ratio of 0.027 for drugs meloxicam (i), piroxicam (ii), and tenoxicam (iii). (b) Arrhenius plots of lipid mixing at *D*/*L* ratio of 0.027 for drugs meloxicam (i), piroxicam (ii), and tenoxicam (iii).

TABLE 3: Different Kinetic and Thermodynamic Parameters, Namely, Activation Energy (E_a), Enthalpy of Activation ($\Delta H^{\ddagger}$), and Entropy of Activation ($\Delta S^{\ddagger}$) of Content Mixing and Lipid Mixing at a Constant Concentration of Oxicam Drugs (*D*/*L* = 0.027)

drug	E_a (kJ mol^{-1})	intercept (A)	$\Delta H^{\ddagger}$ (kJ mol^{-1})	$\Delta S^{\ddagger}$ (J mol^{-1} K^{-1})
		content mixing		
meloxicam	89.050	5.46×10^{11}	88.474	−28.855
piroxicam	49.604	47.79×10^{2}	39.025	−183.122
tenoxicam	66.947	6.19×10^{7}	55.994	−104.394
		lipid mixing		
meloxicam	77.834	3.928×10^{10}	75.253	−50.739
piroxicam	44.171	20.08×10^{4}	41.591	−152.044
tenoxicam	56.522	1.31×10^{7}	53.943	−117.318

expected that lipid mixing will be a faster event in comparison to content mixing, as seen by the rates in Table 2. These results clearly indicate that lipid mixing and content mixing are two different sequential events in the mechanistic pathway of NSAIDs induced membrane fusion, with lipid mixing preceding content mixing. However, it should be mentioned that this is a very simple picture of the fusion process as will be discussed later.

3.4. Calculation of Thermodynamic Parameter. The enthalpy ($\Delta H^{\ddagger}$) and entropy ($\Delta S^{\ddagger}$) of the transition state have been

calculated from eqs 4 and 5 following the transition state theory as proposed by Eyring in 1935, where E_a is the activation energy, N_A is Avogadro's number, h is Planck's constant, and R is the universal gas constant:[26,27]

$$\Delta H^{\ddagger} = E_a - RT \quad (4)$$

$$\Delta H^{\ddagger} = R\ln\left(\frac{AN_A h}{RT}\right) - R \quad (5)$$

The values thus obtained have been tabulated in Table 3, which show a negative value of entropy of activation and a positive value of enthalpy of activation for both content mixing and lipid mixing in the presence of all three oxicam NSAIDs. The unfavorable negative values of $\Delta S^{\ddagger}$ and the positive values of $\Delta H^{\ddagger}$ are expected for a transition state, since the transition state is an unstable state through which the process moves forward toward a more stable product state. For lipid mixing, the transition state moves toward the intermediate hemifused state or to a completely fused state as in the case of content mixing.

4. Discussion

The nature of the fusogenic agents play a crucial role in determining the exact mechanism by which membrane fusion proceeds toward completion. This is because membrane fusion involves the formation of some specific intermediates such as stalks and pores, and each step of the process is controlled by a specific energy barrier. Proteins or peptides that act as fusogenic agents have the capability to supply the crucial structure−energy balance required for the successful fusion event, mostly through the conformational reorganization of their own structure and also by perturbation of the lipid bilayer.[28,29] This advantage of proteins and peptides is not shared by small drug molecules. The little structural reorientation that a typical drug molecule can undergo is not expected to provide enough energy to cross all barriers of the intermediate steps in the fusion process.

For lipidic fusion, where proteins/peptides play no role, introduction of defects or perturbation in the bilayer is known to promote fusion.[30] Defects can make the collision between membranes more inelastic or "sticky" promoting the first step of membrane aggregation in the fusion pathway. This kind of fusion is found to occur in the presence of halothane, the only other drug molecule known to induce membrane fusion at a very high drug to lipid ratio (D/L) of 10.[31] At such a high concentration of drug, the vesicles are overloaded with halothane causing adequate perturbation of the vesicles, like increased headgroup spacing that makes the collision between two vesicles more than enough "sticky" for the promotion of fusion.

Our results on the effect of drug concentration variation on the fusion of DMPC SUVs show that, even at a very low D/L ratio of 0.018, all three oxicam drugs, namely, meloxicam, piroxicam, and tenoxicam, can induce membrane fusion. It should be mentioned that, even though we are using SUVs of DMPC of average diameter of 50−60 nm, spontaneous fusion due to high curvature of the vesicles does not occur under the experimental conditions and time frame used in our study as reflected by the controls.

How small drug molecules like the oxicam NSAIDs can induce membrane fusion at such unusually low D/L ratio is the critical question. Our results on the effect of drug concentration and temperature variation on the fusion process is the first step to answer that question.

The results presented in this study demonstrate the following points:

(1) The oxicam NSAIDs, namely, Mx, Px, and Tx, can induce membrane fusion even for such a low D/L ratio of 0.018 without the aid of any other fusion inducing agent.

(2) The fusion rates for each of the drugs increase with the increase in concentration up to a certain threshold D/L ratio, which is different for the three different drugs. Beyond the threshold value, the rates of fusion decrease since leakage, leading to rupture, competes with the fusion process.

(3) The rates of lipid mixing and content mixing show that for all three drugs, lipid mixing and content mixing are two sequential events with lipid mixing preceding content mixing. This is consistent with the sequential model of membrane fusion, where lipid mixing to form the stalk precedes pore formation leading to content mixing.[32]

(4) Activation energies determined from the linear Arrhenius plots give values less than those in the case of PEG induced fusion of SUVs of diameter ∼45 nm but higher than those of highly curved vesicles of diameter ∼20 nm.[33]

(5) The calculated transition state thermodynamic parameters show both unfavorable enthalpy and entropy contribution that is consistent with the unstable nature of the state.

It is known that, for vesicles with smaller diameter, the activation energy is lowered by increasing the curvature of the vesicles, that is, by increasing the energy of the initial unfused state.[34,35] The size of DMPC vesicles that we used have an average diameter between 50 and 60 nm, which has been estimated from the TEM study. The lower activation energy, both for the lipid mixing and content mixing compared to vesicles of lower diameter of ∼45 nm,[33] is certainly the effect of oxicam NSAIDs. It also demonstrates that, for oxicam NSAIDs, the curvature of vesicles is not the driving force for fusion. It is extremely important to know the mechanism by which these drug molecules bring down the activation energy (E_a) for the intermediate steps promoting a smooth and successful fusion event for such a low D/L ratio.

It is known that membrane perturbation or introduction of defects in the form of any external agents such as any organic molecules or any sort of physical change such as temperature is a cause of lipidic fusion in the absence of proteins.[30,36,37] In our previous work, we have studied the interaction of Mx, Px, and Tx with a DMPC monolayer, spanning a concentration range similar to this study.[38] We have shown that these drugs can perturb the monolayer, such that the monolayer plane is no longer well-defined. This has been explained tentatively by invoking two competitive forces in the overall drug−lipid interaction. An "in plane" force that tends to integrate the drug molecule to the plane formed by the lipid monolayer and the second "out of plane" force that perturbs the drug and the lipid molecules such that the geometry of the monolayer plane is no longer well-defined. The perturbing effect of the drugs could be a possible explanation, how the small drug molecules lower the activation energies of the intermediate steps of the fusion process to lead the process to completion. We are aware that a single exponential description of the time courses and the linear Arrhenius plots fail to give the microscopic details of the mechanism by which oxicam NSAIDs induce membrane fusion. Despite that, this simple description brings out several salient features of the mechanism as mentioned above. It is now clear to us that the mechanism of these drug induced membrane fusions is controlled by the interplay of different physical and chemical parameters of both the participating lipids and the drugs. Here, we have presented the effect of drug concentration

and temperature only while the effect of other parameters has not been completely isolated and deciphered. It is therefore too early for us to make a structure−function analysis of the fusion mediated by the three compounds, and it is difficult to assign a direct correlation of the structure with that of different activation energies of the drugs. Our future studies will aim to dissect the effect of the other parameters on NSAIDs induced membrane fusion process.

5. Conclusion

Membrane fusion induced by oxicam NSAIDs, namely, Mx, Px, and Tx, followed by drug concentration variation and temperature variation, puts forward a simple picture for the fusion pathway with several salient features. These include the identification of lipid mixing and content mixing as two sequential events in the fusion pathway; reduction of activation energy for both lipid mixing and content mixing compared to smaller diameter vesicles promotes the fusion process. This has been explained in terms of the ability of the drugs to perturb lipidic structural arrangements spanning such low drug concentration region as studied here.

Acknowledgment. We acknowledge the help of Mr. Pulak Ray, Mr. Tapan Kumar Ray, and Mr. Ajay Chakrabarti of the Biophysics Division of Saha Institute of Nuclear Physics for their help in transmission electron microscopy.

References and Notes

(1) Hernandez, L. D.; Hoffman, L. R.; Wolfsberg, T. G.; White, J. M. Virus-Cell and Cell-Cell Fusion. *Annu. Rev. Cell Dev. Biol.* **1996**, *12*, 627–661.

(2) Ulrich, A. S.; Otter, M.; Glabe, C. G.; Hoekstra, D. Membrane Fusion is Induced by a Distinct Peptide Sequence of the Sea Urchin Fertilization Protein Bindin. *J. Biol. Chem.* **1998**, *273*, 16748–16755.

(3) Jahn, R.; Lang, T.; Sudhof, T. C. Membrane Fusion. *Cell* **2003**, *112*, 519–533.

(4) Leikina, E.; Markovic, I.; Chernomordik, L. V.; Kozlov, M. M. Delay of Influenza Hemagglutinin Refolding into a Fusion-Competent Conformation by Receptor Binding: A Hypothesis. *Biophys. J.* **2000**, *79*, 1415–1427.

(5) Haque, M. E.; Koppaka, V.; Axelsen, P. H.; Lentz, B. R. Properties and Structures of the Influenza and HIV Fusion Peptides on Lipid Membranes: Implications for a Role in Fusion. *Biophys. J.* **2005**, *89*, 3183–3194.

(6) Chen, E. H.; Olson, E. N. Unveiling the Mechanisms of Cell-Cell Fusion. *Science* **2005**, *308*, 369–373.

(7) Gabrijel, M.; Kreft, M.; Zorec, R. Monitoring Lysosomal Fusion in Electrofused Hybridoma Cells. *BBA-Biomembranes* **2008**, *1778*, 483–490.

(8) Salmons, B.; Güznburg, W. H. Targeting of Retroviral Vectors for Gene Therapy. *Human Gene Ther.* **1993**, *4*, 129–141.

(9) Ogura, A.; Matsuda, J.; Yanagimachi, R. Birth of Normal Young after Electrofusion of Mouse Oocytes with Round Spermatids. *Proc. Natl. Acad. Sci. U.S.A.* **1994**, *91*, 7460–7462.

(10) Coskun, S.; Jaroudi, K. A.; Hollanders, J.; Parhar, R. S.; Al-Sedairy, S. T.; Al-Mohanna, F. A. P-052 Presence of Interleukin-12 and Leukemia Inhibitory Factor in Human Follicular Fluid from Immature and Mature Follicles. *Fertility Sterility* **1997**, *68* (supplement 1), 116–117.

(11) Wakayama, S.; Kishigami, S.; Thuan, N. V.; Ohta, H.; Hikichi, T.; Mizutani, E.; Yanagimachi, R.; Wakayama, T. Propagation of an Infertile Hermaphrodite Mouse Lacking Germ Cells by Using Nuclear Transfer and Embryonic Stem Cell Technology. *Proc. Natl. Acad. Sci. U.S.A.* **2005**, *102*, 29–33.

(12) Lentz, B. R.; Talbot, W.; Lee, J.; Zheng, L.-X. Transbilayer Lipid Redistribution Accompanies Poly(ethylene glycol) Treatment of Model Membranes but Is Not Induced by Fusion. *Biochemistry* **1997**, *36*, 2076–2083.

(13) Cohen, F. S.; Melikyan, G. B. The Energetics of Membrane Fusion from Binding, through Hemifusion, Pore Formation, and Pore Enlargement. *J. Membr. Biol.* **2004**, *199*, 1–14.

(14) Fernandez, I.; Araç, D.; Ubach, J.; Gerber, S. H.; Shin, O.-H.; Gao, Y.; Anderson, R. G. W.; Südhof, T. C.; Rizo, J. Three-Dimensional Structure of the Synaptotagmin 1 C2B-Domain: Synaptotagmin 1 as a Phospholipid-Binding Machine. *Neuron* **2001**, *32*, 1057–1069.

(15) Chakraborty, H.; Mondal, S.; Sarkar, M. Membrane Fusion: A New Function of Non Steroidal Anti-Inflammatory Drugs. *Biophys. Chem.* **2008**, *137*, 28–34.

(16) Chakraborty, H.; Chakraborty, P. K.; Raha, S.; Mandal, P. C.; Sarkar, M. Interaction of Piroxicam with Mitochondrial Membrane and Cytochrome C. *BBA-Biomembranes* **2007**, *1768*, 1138–1146.

(17) Chernomordik, L.; Kozlov, M. M.; Zimmerberg, J. Lipids in Biological Membrane Fusion. *Membr. Biol.* **1995**, *146*, 1–14.

(18) Huang, C. H. Studies on Phosphatidylcholine Vesicles. Formation and Physical Characteristics. *Biochemistry* **1969**, *8*, 344–352.

(19) Chakraborty, H.; Roy, S.; Sarkar, M. Interaction of Oxicam NSAIDs with DMPC Vesicles: Differential Partitioning of Drugs. *Chem. Phys. Lipids* **2005**, *138*, 20–28.

(20) Fiske, C. H.; Subbarow, Y. The Calorimetric Determination of Phosphorous. *J. Biol. Chem.* **1925**, *66*, 375–400.

(21) Wilschut, J.; Düzgüneş, N.; Fraley, R.; Papahadjopoulos, D. Studies on the Mechanism of Membrane Fusion: Kinetics of Calcium Ion Induced Fusion of Phosphatidylserine Vesicles Followed by a New Assay for Mixing of Aqueous Vesicle Contents. *Biochemistry* **1980**, *19*, 6011–6021.

(22) Düzgüneş, N.; Wilschut, J. Fusion Assays Monitoring Intermixing of Aqueous Contents. In *Methods Enzymology*; Düzgüneş, N., Ed.; Academic Press, Inc.: San Diego, CA, 1993; Vol. 220, pp 3−14.

(23) Struck, D. K.; Hoekstra, D.; Pagano, R. E. Use of Resonance Energy Transfer to Monitor Membrane Fusion. *Biochemistry* **1981**, *20*, 4093–4099.

(24) Hoekstra, D.; Düzgüneş, N. Lipid Mixing Assays to Determine Fusion in Liposome Systems. In *Methods Enzymology*; Düzgüneş, N., Ed.; Academic Press, Inc.: San Diego, CA, 1993; Vol. 220, pp 15−32.

(25) Düzgüneş, N.; Bagatolli, L. A.; Meers, P.; Oh, Y.-K.; Straubinger, R. M. Fluorescence Methods in Lipid Research. In *Liposomes: A Practical Approach*, 2nd ed.; Torchilin, V., Weissig, V., Eds.; Oxford University Press: New York; pp 113−116.

(26) *Fundamentals of Enzyme Kinetics*, 2nd ed.; Cornish-Bowden, A., Ed.; Portland Press: London, 1995; pp 14−16.

(27) Cornish-Bowden, A. Enthalpy-Entropy Compensation: A Phantom Phenomenon. *J. Biosci.* **2002**, *27*, 121–126.

(28) Kozlov, M. M.; Chernomordik, L. V. A Mechanism of Protein-Mediated Fusion: Coupling between Refolding of the Influenza Hemagglutinin and Lipid Rearrangements. *Biophys. J.* **1998**, *75*, 1384–1396.

(29) Lentz, B. R.; Malinin, V.; Haque, M. E.; Evans, K. Protein Machines and Lipid Assemblies: Current Views of Cell Membrane Fusion. *Curr. Opin. Struct. Biol.* **2000**, *10*, 607–615.

(30) Cevc, G.; Richardson, H. Lipid Vesicles and Membrane Fusion. *Adv. Drug Delivery Rev.* **1999**, *38*, 207–232.

(31) Swift, J. L.; Carnini, A.; Dahms, T. E. S.; Cramb, D. T. Anesthetic-Enhanced Membrane Fusion Examined Using Two-Photon Fluorescence Correlation Spectroscopy. *J. Phys. Chem. B* **2004**, *108*, 11133–11138.

(32) Weinreb, G.; Lentz, B. R. Analysis of Membrane Fusion as a Two-State Sequential Process: Evaluation of the Stalk Model. *Biophys. J.* **2007**, *92*, 4012–4029.

(33) Evans, K. O.; Lentz, B. R. Kinetics of Lipid Rearrangements during Poly(ethylene glycol)-Mediated Fusion of Highly Curved Unilameller Vesicles. *Biochemistry* **2002**, *41*, 1241–1249.

(34) Talbot, W. A.; Zheng, L.-X.; Lentz, B. R. Acyl Chain Unsaturation and Vesicle Curvature Alter Outer Leaflet Packing and Promote Poly(ethylene glycol)-Mediated Membrane Fusion. *Biochemistry* **1997**, *36*, 5827–5836.

(35) Lee, J. K.; Lentz, B. R. Secretory and Viral Fusion May Share Mechanistic Events with Fusion between Curved Lipid Bilayers. *Proc. Natl. Acad. Sci. U.S.A.* **1998**, *95*, 9274–9279.

(36) Wieclaw, K.; Korchowiec, B.; Corvis, Y.; Korchowiec, J.; Guermouche, H.; Rogalska, E. Meloxicam and Meloxicam-β-Cyclodextrin Complex in Model Membranes: Effects on the Properties and Enzymatic Lypolysis of Phospholipid Monolayers in Relation to Anti-Inflammatory Activity. *Langmuir* **2009**, *25*, 1417–1426.

(37) Bentz, J. Intermediate and Kinetics of Membrane Fusion. *Biophys. J.* **1992**, *63*, 448–459.

(38) Kundu, S.; Chakraborty, H.; Sarkar, M.; Datta, A. Interaction of Oxicam NSAIDs with Lipid Monolayer: Anomalous Dependence on Drug Concentration. *Colloids Surf. B: Biointerfaces* **2009**, *70*, 157–161.

JP9069527